Geosciences 2018, 8(2): 21-31
DOI: 10.5923/j.geo.20180802.01

On the Seismic Hazard in Himachal Pradesh and Uttarakhand States

D. Shanker*, Shubham

Indian Institute of Technology Roorkee, Department of Earthquake Engineering, Roorkee, Uttarakhand, India

Abstract Seismic hazard analysis involves the quantitative estimation of ground shaking at a particular site or for a particular region. In the present study Deterministic Seismic Hazard Analysis (DSHA) has been carried out for the states of Himachal Pradesh & Uttarakhand. The study region is one of the most seismically active regions of western part of Himalaya, India and there are numerous major seismic faults present in this region. Eighty-nine seismo-tectonic sources in and around Himachal Pradesh & Uttarakhand were identified. Using an appropriate attenuation model the peak horizontal accelerations, peak vertical accelerations and ratios of peak vertical to horizontal accelerations were computed. For this purpose the study region was divided into grids of 0.5° by 0.5°. The estimated peak horizontal accelerations vary from 0.02g to 0.60g and peak vertical accelerations vary from 0.01g to 0.47g. The ratios of horizontal to vertical accelerations vary from 3.60 to 1.28. This variation seems to be more realistic because it takes into account the effect of large number of tectonic features that may rupture causing earthquakes. The PGA contour maps prepared for the region show that larger Peak Ground Accelerations are present in the region where there is a higher density of larger faults and vice versa.

Keywords Deterministic Seismic Hazard Analysis (DSHA), Peak horizontal accelerations, Peak vertical accelerations

1. Introduction

Destructive effects of earthquakes is becoming alarming day by day because of growth in population, the rapid rate of industrialization, the large scale engineering activities and their impact on the environment, which now call for increased efforts to minimize resulting seismic hazards. The human population and the extent of built- up areas (cities etc.) are directly related, and, at present, both are increasing in a big way. Also the effects of ground motion (vibrations) on various structures as well as on human beings have become a great concern for the society. It is felt that an assessment of seismic hazards is fundamentally a predictive effort where attempts are made to forecast the earthquake effects in a region in terms of ground motion (shanking). Therefore, somehow or other, the seismic hazard assessment is analogous to the long-term earthquake prediction. In a real sense, it is a challenge to before the geoscientific community to improve the quantification of earthquake hazards for societal benefits. The local geological and soil conditions can profoundly influence all of the characteristics – amplitude, frequency content, and duration – of strong ground motion. Significant earthquake damage and loss of life has been directly related to the effect of local site condition in several recent earthquakes (eg., 1985 Mexico earthquake, 1989 Loma Prieta Earthquake, 1994 Northridge, 1995 Kobe Earthquake, and Bhuj earthquake 2001) which effects play an important role in earthquake resistant design [3]. local site condition related damage are very essential component of a comprehensive assessment of seismic hazard and are attributed to geotechnical / geophysical characteristics of soil overburden closure to the ground. There is a clear role for geological and geotechnical data in evaluating the ground motions and in turn in the study of seismic hazard.

* Corresponding author:
dayasfeq@iitr.ac.in (D. Shanker)
Published online at http://journal.sapub.org/geo

2. Characteristics of Study Region

The considered region falls within 29°N - 33°N latitude and 75°E - 81°E longitude and is located in Himalayan range (Fig. 1). This region comes under the Zone IV (severe) and Zone V (very severe) of the seismic zoning map of India (IS: 1893-2002) with damage intensity of VIII and IX, respectively [8]. It is seismically a very active region and cascades in the zone of continental collision of the Indian and Eurasian plates [5]. The seismic activity of this area is closely associated with the several active faults running nearby and the dynamic regional tectonic features. The region is in the lap of Himalayas, and the Himalayan orogeny resulted in the formation of a large number of major faults in this region. Seismotectonics of the region is related to the regional tectonic features like thrusts and faults, their

interactions and clustering of epicentres at places. Thus, the frequent seismic activities observed in this region are due to ruptures at these thrust faults formed by the subduction of the Indian plate below the slow moving Eurasian plate [5]. Some of these prominent faults are the Main Frontal Thrust (MFT) [11, 12] the north-west-south-east trending Main Boundary Thrust (MBT) and Main Central Thrust (MCT) running parallel to Himalayas and other local transverse faults across the area. A highly devastating earthquake of magnitude 7.8 on the Richter scale occurred in 1905 within the study area. Despite the seismicity, the increase in the population in the high seismicity regions of this state has led to increase in the seismic vulnerability. For the present study, deterministic seismic hazard assessment have been carried out.

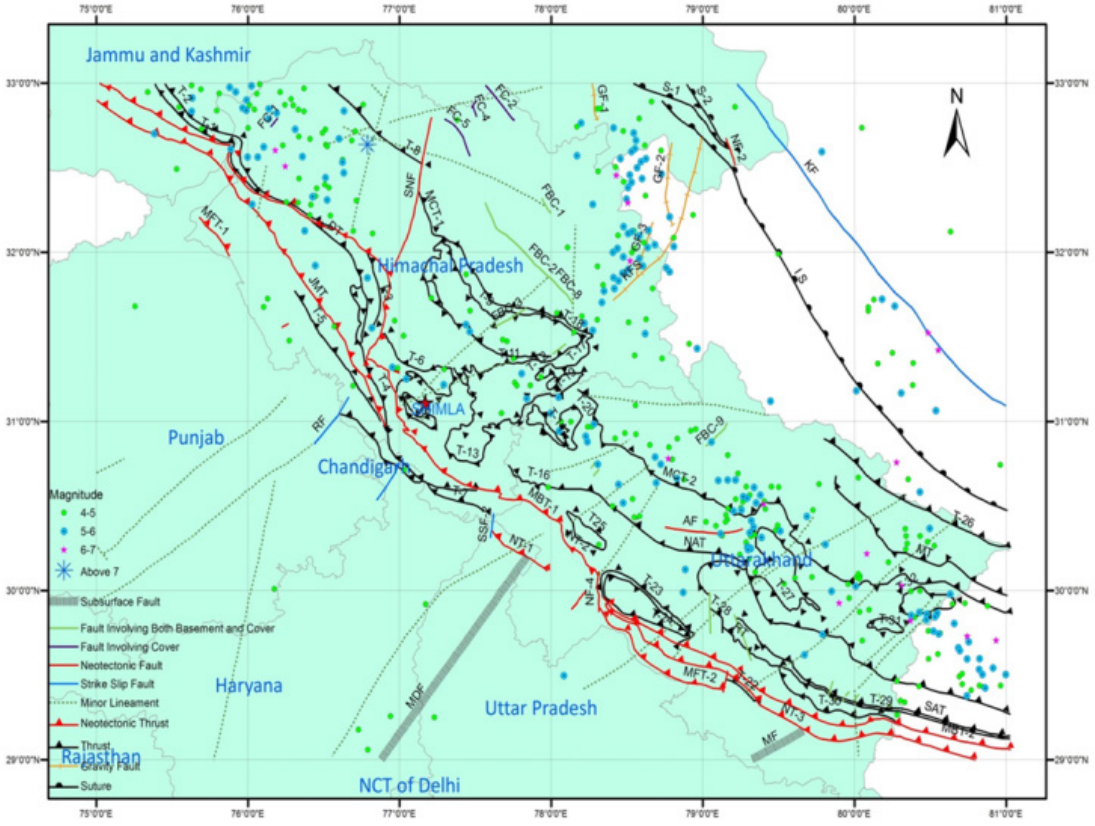

Figure 1. Seismotectonic map of the considered region (after [7]) in the study region

3. Method of Analyses

3.1. Deterministic Seismic Hazard Assessment of the Study Region

3.1.1. Identification of Seismotectonic Sources

Based on regional seismicity and tectonic setting of the region under study, Eighty nine seismotectonic sources have been identified which are linear in character. These sources are listed in Table 1 and plotted using Arc GIS 10.1.

Table 1. Details of the seismotectonic sources in the study area

S.No.	SOURCE NAME	TYPE OF SOURCE
1	Main Boundary Thrust-1(MBT-1)	Neotectonic Thrust Fault
2	Jwala Mukhi Thrust(JMT)	Neotectonic Thrust Fault
3	Main Frontal Thrust(MFT-1)	Neotectonic Thrust Fault
4	NT-1	Neotectonic Thrust Fault
5	NT-2	Neotectonic Thrust Fault
6	Main Frontal Thrust-2(MFT-2)	Neotectonic Thrust Fault
7	Main Boundary Thrust-2(MBT-2)	Neotectonic Thrust Fault
8	NT-3	Neotectonic Thrust Fault
9	T-1	Thrust Fault
10	T-2	Thrust Fault
11	T-3	Thrust Fault
12	Drang Thrust(DT)	Thrust Fault
13	T-4	Thrust Fault
14	T-5	Thrust Fault
15	T-6	Thrust Fault
16	T-7	Thrust Fault
17	T-8	Thrust Fault
18	Main Central Thrust-1(MCT-1)	Thrust Fault
19	T-9	Thrust Fault
20	T-10	Thrust Fault
21	T-11	Thrust Fault

22	T-12	Thrust Fault
23	T-13	Thrust Fault
24	T-14	Thrust Fault
25	T-15	Thrust Fault
26	T-16	Thrust Fault
27	T-17	Thrust Fault
28	T-18	Thrust Fault
29	T-19	Thrust Fault
30	T-20	Thrust Fault
31	Main Central Thrust-2(MCT-2)	Thrust Fault
32	North Almora Thrust(NAT)	Thrust Fault
33	T-21	Thrust Fault
34	T-22	Thrust Fault
35	T-23	Thrust Fault
36	T-24	Thrust Fault
37	T25	Thrust Fault
38	T-26	Thrust Fault
39	Martoli Thrust(MT)	Thrust Fault
40	T-27	Thrust Fault
41	T-28	Thrust Fault
42	RT	Thrust Fault
43	South Almora Thrust(SAT)	Thrust Fault
44	T-29	Thrust Fault
45	T-30	Thrust Fault
46	T-31	Thrust Fault
47	T-32	Thrust Fault
48	SSF-1	Strike Slip Fault
49	Ropor Fault(RF)	Strike Slip Fault
50	SSF-2	Strike Slip Fault
51	Karakoram Fault(KF)	Strike Slip Fault
52	FBC-1	Fault Involving Both Basement and Cover
53	FBC-2	Fault Involving Both Basement and Cover
54	FBC-3	Fault Involving Both Basement and Cover
55	FBC-4	Fault Involving Both Basement and Cover
56	FBC-5	Fault Involving Both Basement and Cover
57	FBC-6	Fault Involving Both Basement and Cover
58	FBC-7	Fault Involving Both Basement and Cover
59	FBC-8	Fault Involving Both Basement and Cover
60	FBC-9	Fault Involving Both Basement and Cover
61	FBC-10	Fault Involving Both Basement and Cover
62	FBC-11	Fault Involving Both Basement and Cover
63	FBC-12	Fault Involving Both Basement and Cover
64	FBC-13	Fault Involving Both Basement and Cover
65	FBC-14	Fault Involving Both Basement and Cover
66	FBC-15	Fault Involving Both Basement and Cover
67	FBC-16	Fault Involving Both Basement and Cover
68	FBC-17	Fault Involving Both Basement and Cover
69	FC-1	Fault involving Cover
70	FC-2	Fault involving Cover
71	FC-3	Fault involving Cover
72	FC-4	Fault involving Cover
73	FC-5	Fault involving Cover
74	NF-1	Neotectonic Fault
75	Sunda Nagar Fault(SNF)	Neotectonic Fault
76	NF-2	Neotectonic Fault
77	NF-3	Neotectonic Fault
78	NF-4	Neotectonic Fault
79	NF-5	Neotectonic Fault
80	Alaknanda Fault(AF)	Neotectonic Fault
81	Mahendragarh Dehradun Fault(MDF)	Subsurface Fault
82	Moradabad Fault(MF)	Subsurface Fault
83	GF-1	Gravity Fault
84	GF-2	Gravity Fault
85	Kaurik Fault System(KFS)	Gravity Fault
86	GF-3	Gravity Fault
87	Indus Suture(I S)	Suture
88	S-1	Suture
89	S-2	Suture

3.1.2. Estimation of Maximum Magnitude of Sources and Depth or Energy Release

There are two methods of calculating expected magnitude or assigning maximum magnitude to any fault.

a) ***Based on past seismicity*:** This method uses observed maximum magnitude in a seismic zone from the earthquake catalogue. This is not an efficient method because there are some of the fault which do not have any significant earthquake present on them, which is responsible for ground motion. This doesn't mean that they cannot trigger any future earthquakes.

b) ***Based on dimensions of rupture*:** In this method the concept of fault rupture length has been utilized. Worldwide earthquake studies have shown that faults do not rupture over the entire lengths or areas during individual event.

Adopting the general assumption based on world wide data that 1/3 to 1/2 of the total length of fault would rupture producing the maximum earthquake and using the following

relationships between the surface rupture length (L) and earthquake magnitude for reverse, strike slip, and normal faults, the moment magnitude (M_W) for each seismotectonic source has been computed [13].

$M_W = 5.16 + 1.12\log L$ (Strike Slip Fault)

$M_W = 5.00 + 1.22\log L$ (Reverse Fault)

$M_W = 4.86 + 1.32\log L$ (Normal Fault)

Adopting the above relationships, the maximum magnitude and rupture width, for various seismotectonic sources have been computed and are listed in Table 2.

Table 2. Seismotectonic sources and corresponding fault length, Rupture Length, maximum magnitude Rupture width (R_W), Depth to the zone of energy release (D_Z)

S.No.	SOURCE NAME	Fault Type	FAULT LENGTH (km)	RUPTURE LENGTH (km)	Magnitude M_w	RUPTURE WIDTH R_W(km)	D_Z (km)
1	MBT-1	RF	472.679406	157.55980	7.68	28.03	6.63
2	JMT	RF	292.420579	97.47353	7.43	23.31	6.02
3	MFT-1	RF	32.180590	10.72686	6.26	9.84	16.73
4	NT-1	RF	45.649790	15.21660	6.44	11.24	16.55
5	NT-2	RF	52.370555	17.45685	6.52	11.92	16.46
6	MFT-2	RF	103.540521	34.51351	6.88	15.55	5.01
7	MBT-2	RF	289.520226	96.50674	7.42	23.14	5.99
8	NT-3	RF	273.268453	91.08948	7.39	22.64	5.93
9	T-1	RF	105.225015	35.07500	6.88	15.55	5.01
10	T-2	RF	152.047260	50.68242	7.08	18.01	5.33
11	T-3	RF	53.352289	17.78410	6.53	12.01	16.45
12	DT	RF	94.319669	31.43989	6.83	14.98	16.06
13	T-4	RF	186.927368	62.30912	7.19	19.53	5.53
14	T-5	RF	101.771729	33.92391	6.87	15.43	5.00
15	T-6	RF	132.598840	44.19961	7.01	17.11	5.21
16	T-7	RF	118.909711	39.63657	6.95	16.37	5.12
17	T-8	RF	78.651345	26.21712	6.73	13.92	16.20
18	MCT-1	RF	130.011494	43.33716	7.00	16.98	5.20
19	T-9	RF	249.817324	83.27244	7.34	21.82	5.82
20	T-10	RF	23.002337	7.66745	6.08	8.62	16.88
21	T-11	RF	94.769922	31.58997	6.83	14.98	16.06
22	T-12	RF	41.896887	13.96563	6.40	10.91	16.59
23	T-13	RF	176.407139	58.80238	7.16	19.11	5.47
24	T-14	RF	80.486629	26.82888	6.74	14.02	16.19
25	T-15	RF	97.961227	32.65374	6.85	15.21	4.97
26	T-16	RF	36.885118	12.29504	6.33	10.37	16.66
27	T-17	RF	73.189976	24.39666	6.69	13.51	16.25
28	T-18	RF	47.870366	15.95679	6.47	11.49	16.51
29	T-19	RF	52.209997	17.40333	6.51	11.84	16.47
30	T-20	RF	73.079781	24.35993	6.69	13.51	16.25
31	MCT-2	RF	369.447808	123.14927	7.55	25.47	6.30
32	NAT	RF	351.479821	117.15994	7.52	24.91	6.22
33	T-21	RF	53.173910	17.72464	6.52	11.92	16.46
34	T-22	RF	24.988588	8.32953	6.12	8.88	16.85
35	T-23	RF	103.297214	34.43240	6.88	15.55	5.01
36	T-24	RF	142.482022	47.49401	7.05	17.62	5.28
37	T25	RF	75.991061	25.33035	6.71	13.72	16.23
38	T-26	RF	138.540138	46.18005	7.03	17.36	5.25
39	MT	RF	147.078253	49.02608	7.06	17.75	5.30
40	T-27	RF	172.892035	57.63068	7.15	18.97	5.45
41	T-28	RF	19.851026	6.61701	6.00	8.13	16.95
42	RT	RF	25.178248	8.39275	6.13	8.95	16.84

S.No.	SOURCE NAME	Fault Type	FAULT LENGTH (km)	RUPTURE LENGTH (km)	Magnitude M_w	RUPTURE WIDTH R_W(km)	D_Z (km)
43	SAT	RF	201.473078	67.15769	7.23	20.12	5.60
44	T-29	RF	181.477001	60.49233	7.17	19.25	5.49
45	T-30	RF	94.781917	31.59397	6.83	14.98	16.06
46	T-31	RF	54.365782	18.12193	6.54	12.10	16.43
47	T-32	RF	90.369013	30.12300	6.80	14.66	16.10
48	SSF-1	SS	28.294091	9.43136	6.25	9.77	13.11
49	RF	SS	38.041202	12.68040	6.40	10.91	12.54
50	SSF-2	SS	16.313835	5.43795	5.98	8.01	14.00
51	KF	SS	271.849110	90.61637	7.35	21.98	13.99
52	FBC-1	RF	11.608156	3.86939	5.72	6.61	17.14
53	FBC-2	RF	65.755496	21.91850	6.64	13.03	16.31
54	FBC-3	RF	23.536489	7.84550	6.09	8.69	16.88
55	FBC-4	RF	27.302559	9.10085	6.17	9.21	16.81
56	FBC-5	RF	5.670934	1.89031	5.34	5.00	17.35
57	FBC-6	RF	5.739762	1.91325	5.34	5.00	17.35
58	FBC-7	RF	10.854242	3.61808	5.68	6.42	17.17
59	FBC-8	RF	21.739126	7.24638	6.05	8.43	16.91
60	FBC-9	RF	20.880068	6.96002	6.03	8.31	16.93
61	FBC-10	RF	32.427363	10.80912	6.26	9.84	16.73
62	FBC-11	RF	10.601084	3.53369	5.67	6.37	17.18
63	FBC-12	RF	2.768612	0.92287	4.96	3.78	17.51
64	FBC-13	RF	2.154844	0.71828	4.82	3.41	17.56
65	FBC-14	RF	3.792477	1.26416	5.12	4.25	17.45
66	FBC-15	RF	5.490601	1.83020	5.32	4.92	17.36
67	FBC-16	RF	4.476888	1.49230	5.21	4.54	17.41
68	FBC-17	RF	3.534898	1.17830	5.09	4.16	17.46
69	FC-1	RF	7.231397	2.41047	5.47	5.50	17.29
70	FC-2	RF	29.410776	9.80359	6.21	9.49	16.77
71	FC-3	RF	5.838687	1.94623	5.35	5.04	17.35
72	FC-4	RF	7.608445	2.53615	5.49	5.58	17.28
73	FC-5	RF	30.095242	10.03175	6.22	9.56	16.76
74	NF-1	SS	4.921401	1.64047	5.40	5.22	15.39
75	SNF	SS	101.413849	33.80462	6.87	15.43	10.72
76	NF-2	SS	18.626655	6.20888	6.05	8.43	13.78
77	NF-3	SS	15.655488	5.21850	5.96	7.89	14.05
78	NF-4	SS	26.753763	8.91792	6.22	9.56	13.22
79	NF-5	SS	14.629062	4.87635	5.93	7.72	14.14
80	AF	SS	50.098820	16.69961	6.53	12.01	11.99
81	MDF	SS	163.235688	54.41190	7.10	18.28	12.14
82	MF	SS	37.708774	12.56959	6.39	10.83	12.58
83	GF-1	NF	25.167492	8.38916	6.08	8.62	13.69
84	GF-2	NF	55.485859	18.49529	6.53	12.01	11.99
85	KFS	NF	124.771769	41.59059	7.00	16.98	11.49
86	GF-3	NF	37.580559	12.52685	6.31	10.21	12.89
87	I S	RF	352.365920	117.45531	7.53	25.10	15.55
88	S-1	RF	76.292255	25.43075	6.71	13.72	16.23
89	S-2	RF	48.110901	16.03697	6.47	11.49	16.51

3.1.3. Computational Steps

Computations of the maximum horizontal ground acceleration and maximum vertical ground acceleration at a given point have been carried out using four softwares, namely Arc Info GIS 10.1, Arc View GIS 10.1, MS Excel and Surfer 13. The steps involved in the computation of maximum horizontal acceleration and vertical acceleration are briefly described below:

- All the tectonic features and earthquake epicenters lying between latitude 29° N to 33° N and longitude 75° E to 81° E were identified and digitized in Arc View GIS 10.1. For this SEISAT 5 & 6 from Seismotectonic Atlas of India [7] were scanned and seismotectonic maps were prepared. Using these digitized seismotectonic maps a composite seismotectonic map was prepared indicating seismic sources in terms of faults, lineaments and other geological structures. For computing maximum magnitude of various sources their lengths were estimated.
- The study area lies within latitude 29° N to 33° N and longitude 75° E to 81° E. The area was divided into small grids, each grid having a dimension of 0.5° latitude by 0.5° longitude. Center of each grid is taken as a site for the purpose of calculating ground motion parameter.
- For each site following calculations were made:
  - The closest distance to all seismic sources (faults) were computed using Arc Info GIS 10.1
  - These closest distances were combined with the vertical distances showing the depth of energy release to compute the distance to the zone of energy release. Using these distances to the zone of energy release and maximum magnitudes assigned to various seismotectonic sources, the peak horizontal ground accelerations and vertical accelerations for the sites were computed adopting the prescribed attenuation relationship.
  - The highest of those acceleration values was taken to represent the acceleration at the site under consideration.

The above steps were repeated for all the grid points and the highest acceleration value at the center of each grid was taken for preparing contour maps showing the variation of PGA. The contour map was prepared using Surfer 13.

Knowing the M_w, the rupture width (R_W) for each source is calculated using following relationship [13]

$$\text{Log}\,(R_W) = -1.01 + 0.32M_W$$

For calculating the depth of energy release (D_Z) General Focal Depth (GFD) of 15 km has been taken because the reported focal depths of moderate earthquakes in this region generally fall in range of 10 km to 20 km, and non seismogenic depth (NSD) is taken as 3 km [6]. The dip angle (α) is taken as 15° for thrust type seismotectonic sources, and 90° for normal and strike slip type sources. The depth of energy release (D_Z) has been computed using the following relationship:

$D_Z = \text{NSD} + \text{GFD} - (R_W/2)\sin\alpha$ When $R_W < \text{GFD}$

$D_Z = \text{NSD} + (R_W/2)\sin\alpha$ When $R_W \geq \text{GFD}$

The distance to the zone of energy release (De) is estimated using the depth to the zone of energy release (Dz) and the epicentral distance (Ep) as:

$$D_e = (Ep^2 + Dz^2)^{0.5}$$

The attenuation relationship developed by [1] has been used to compute both peak horizontal acceleration (a_h) and peak vertical acceleration (a_v)

$$\begin{aligned} log_{10}a_h(g) = {} & -0.62 + 0.177M \\ & - 0.982\, log_{10}(r + e^{0.284M}) + 0.132F \\ & - 0.0008Er \\ log_{10}a_v(g) = {} & -1.15 + 0.245M \\ & - 1.096\, log_{10}(r + e^{0.256M}) + 0.096F \\ & - 0.0011Er \end{aligned}$$

4. Computational Results

For conducting Deterministic Seismic Hazard Assessment eighty nine potential seismic line sources were delineated based on the major tectonic features mapped in the study area and observed seismicity patterns. The area was divided into small grids, each grid having a dimension of 0.5° latitude by 0.5° longitude. Center of each grid is taken as a site for the purpose of calculating ground motion parameter. The attenuation relationship developed by [1] has been used to compute both peak horizontal acceleration (ah) and peak vertical acceleration (av). The expected ratios of peak vertical to peak horizontal accelerations (av/ah) have also been computed. The maximum value of peak horizontal and vertical accelerations computed at the center of each grid point, along with the ratio av/ah and the source that has made maximum contribution is listed in Table 3.

5. Discussion and Conclusions

The most extensively used and studied parameter of strong ground motion earthquake records is peak ground acceleration, specially its horizontal component. At the distance beyond which surface waves appear, the vertical component is generally smaller and its frequency is higher compared to horizontal components. The pair of orthogonal horizontal component records (NS-EW) will be randomly oriented with respect to the direction of the progress of the waves and will usually possess comparable amplitudes. The component in the direction of wave propagation is generally larger. Experienced showed that on an average the peak ground acceleration is not so much affected by geology in comparison to the peak horizontal velocity and displacement. The velocity and displacement are found to be larger on soft rock sites. The peak ground acceleration is assocated with higher frequencies on hard rock sites compared to soft rock sites. Also the velocity and displacements are more sensitive to changes in the value of modules of elasticity. The presence

of shallow soft soil layers will amplify the low frequency components (Horizontal) and attenuate high frequency components (vertical). The effect is more pronounced away from the epicenter but will be within 25-30% [2]. It has been also observed that peak ground acceleration is expected to be 15-25% higher for reverse faults compared to strike-slip faults [2]. Additionally, azimuth of the site with respect to the strike of the fault is important. In general at comparable distances the peak horizontal acceleration may be higher in the direction of about 600 to the strike of the fault [2].

Table 3. Computed Peak horizontal accelerations (A_h (g)), peak vertical accelerations (A_v (g)), and ratios of A_h/A_v

S.No.	Latitude (°N)	Longitude (°E)	PGA-Ah(g)	PGA-Av(g)	Ah/Av	Source
1	32.75	75.75	0.46	0.32	1.44	T-2
2	32.75	76.25	0.27	0.14	1.93	FC-1
3	32.75	76.75	0.22	0.13	1.69	T-8
4	32.75	77.25	0.22	0.14	1.57	SNF
5	32.75	77.75	0.22	0.14	1.57	SNF
6	32.75	78.25	0.36	0.10	3.60	S-2
7	32.75	78.75	0.27	0.17	1.59	I S
8	32.75	79.25	0.23	0.14	1.64	KF
9	32.75	79.75	0.42	0.12	3.50	S-2
10	32.75	80.25	0.07	0.04	1.75	KF
11	32.75	80.75	0.04	0.02	2.00	KF
12	32.25	75.75	0.31	0.18	1.72	MFT-1
13	32.25	76.25	0.60	0.47	1.28	MBT-1
14	32.25	76.75	0.27	0.18	1.50	MBT-1
15	32.25	77.25	0.41	0.28	1.46	MCT-1
16	32.25	77.75	0.25	0.14	1.79	FBC-2
17	32.25	78.25	0.12	0.05	2.40	FBC-1
18	32.25	78.75	0.43	0.32	1.34	GF-2
19	32.25	79.25	0.29	0.19	1.53	I S
20	32.25	79.75	0.34	0.26	1.31	KF
21	32.25	80.25	0.13	0.08	1.63	KF
22	32.25	80.75	0.06	0.03	2.00	KF
23	31.75	75.75	0.13	0.06	2.17	MFT-1
24	31.75	76.25	0.41	0.27	1.52	T-5
25	31.75	76.75	0.41	0.28	1.46	T-4
26	31.75	77.25	0.43	0.30	1.43	T-9
27	31.75	77.75	0.35	0.22	1.59	MCT-1
28	31.75	78.25	0.15	0.07	2.14	FBC-8
29	31.75	78.75	0.14	0.09	1.56	KFS
30	31.75	79.25	0.15	0.09	1.67	I S
31	31.75	79.75	0.27	0.18	1.50	I S
32	31.75	80.25	0.22	0.16	1.38	KF
33	31.75	80.75	0.11	0.07	1.57	KF
34	31.25	75.75	0.07	0.03	2.33	JMT
35	31.25	76.25	0.50	0.37	1.35	MBT-1
36	31.25	76.75	0.48	0.34	1.41	JMT
37	31.25	77.25	0.35	0.23	1.52	T-6
38	31.25	77.75	0.28	0.17	1.65	T-9
39	31.25	78.25	0.36	0.25	1.44	MCT-2
40	31.25	78.75	0.13	0.07	1.86	MCT-2
41	31.25	79.25	0.10	0.05	2.00	I S

S.No.	Latitude (°N)	Longitude (°E)	PGA-Ah(g)	PGA-Av(g)	Ah/Av	Source
42	31.25	79.75	0.21	0.13	1.62	I S
43	31.25	80.25	0.21	0.13	1.62	I S
44	31.25	80.75	0.22	0.16	1.38	KF
45	30.75	75.75	0.05	0.02	2.50	T-7
46	30.75	76.25	0.10	0.06	1.67	RF
47	30.75	76.75	0.27	0.16	1.69	T-7
48	30.75	77.25	0.49	0.37	1.32	MBT-1
49	30.75	77.75	0.25	0.16	1.56	MBT-1
50	30.75	78.25	0.29	0.19	1.53	MCT-2
51	30.75	78.75	0.36	0.24	1.50	MCT-2
52	30.75	79.25	0.19	0.11	1.73	MCT-2
53	30.75	79.75	0.26	0.16	1.63	MT
54	30.75	80.25	0.24	0.14	1.71	T-26
55	30.75	80.75	0.24	0.15	1.60	I S
56	30.25	75.75	0.04	0.02	2.00	MBT-1
57	30.25	76.25	0.06	0.03	2.00	MBT-1
58	30.25	76.75	0.09	0.05	1.80	MBT-1
59	30.25	77.25	0.14	0.07	2.00	T-7
60	30.25	77.75	0.20	0.11	1.82	NT-1
61	30.25	78.25	0.22	0.13	1.69	T-25
62	30.25	78.75	0.48	0.35	1.37	NAT
63	30.25	79.25	0.40	0.28	1.43	NAT
64	30.25	79.75	0.39	0.27	1.44	MCT-2
65	30.25	80.25	0.46	0.31	1.48	MT
66	30.25	80.75	0.32	0.20	1.60	T-26
67	29.75	75.75	0.03	0.01	3.00	MBT-1
68	29.75	76.25	0.04	0.02	2.00	MBT-1
69	29.75	76.75	0.06	0.03	2.00	MDF
70	29.75	77.25	0.15	0.09	1.67	MDF
71	29.75	77.75	0.14	0.09	1.56	MDF
72	29.75	78.25	0.23	0.14	1.64	NT-3
73	29.75	78.75	0.47	0.34	1.38	MBT-2
74	29.75	79.25	0.40	0.27	1.48	SAT
75	29.75	79.75	0.49	0.36	1.36	NAT
76	29.75	80.25	0.21	0.12	1.75	T-31
77	29.75	80.75	0.23	0.15	1.53	MCT-2
78	29.25	75.75	0.02	0.01	2.00	MBT-1
79	29.25	76.25	0.05	0.03	1.67	MDF
80	29.25	76.75	0.12	0.07	1.71	MDF
81	29.25	77.25	0.17	0.11	1.55	MDF
82	29.25	77.75	0.07	0.04	1.75	MDF
83	29.25	78.25	0.09	0.05	1.80	NT-3
84	29.25	78.75	0.16	0.09	1.78	MFT-2
85	29.25	79.25	0.28	0.18	1.56	NT-3
86	29.25	79.75	0.49	0.35	1.40	MBT-2
87	29.25	80.25	0.47	0.34	1.38	MBT-2
88	29.25	80.75	0.38	0.25	1.52	SAT

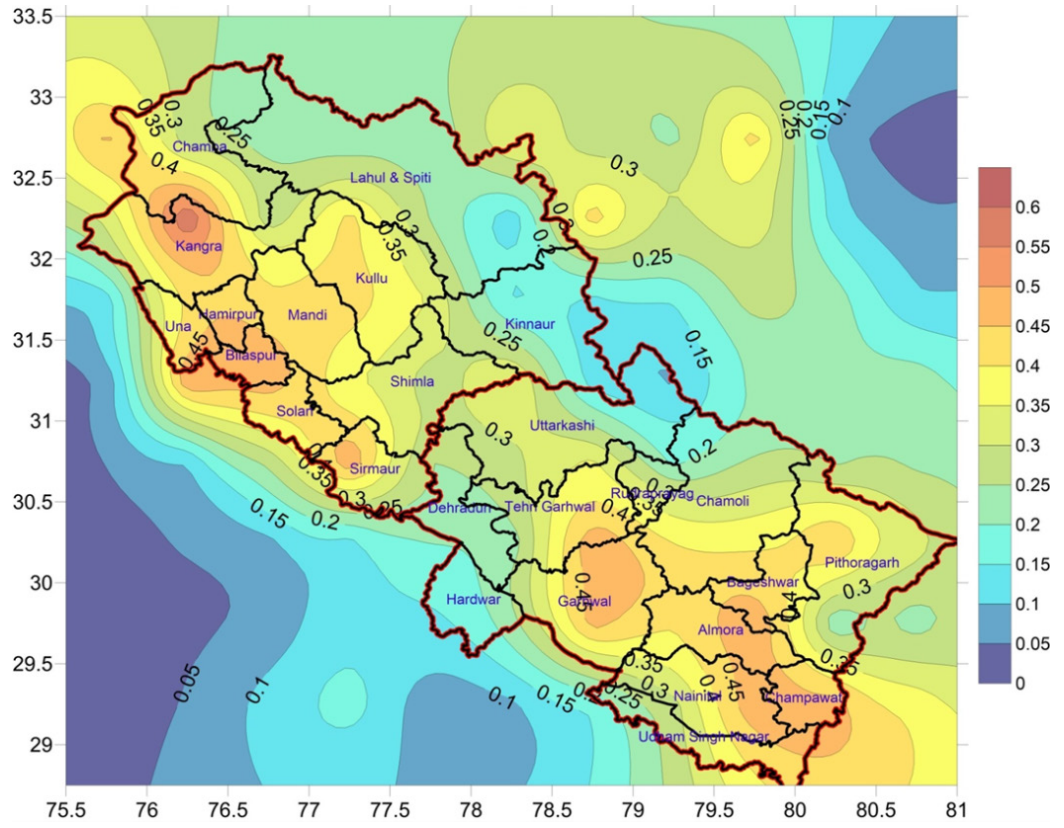

Figure 2. Contour map showing variation of peak horizontal accelerations in the study region

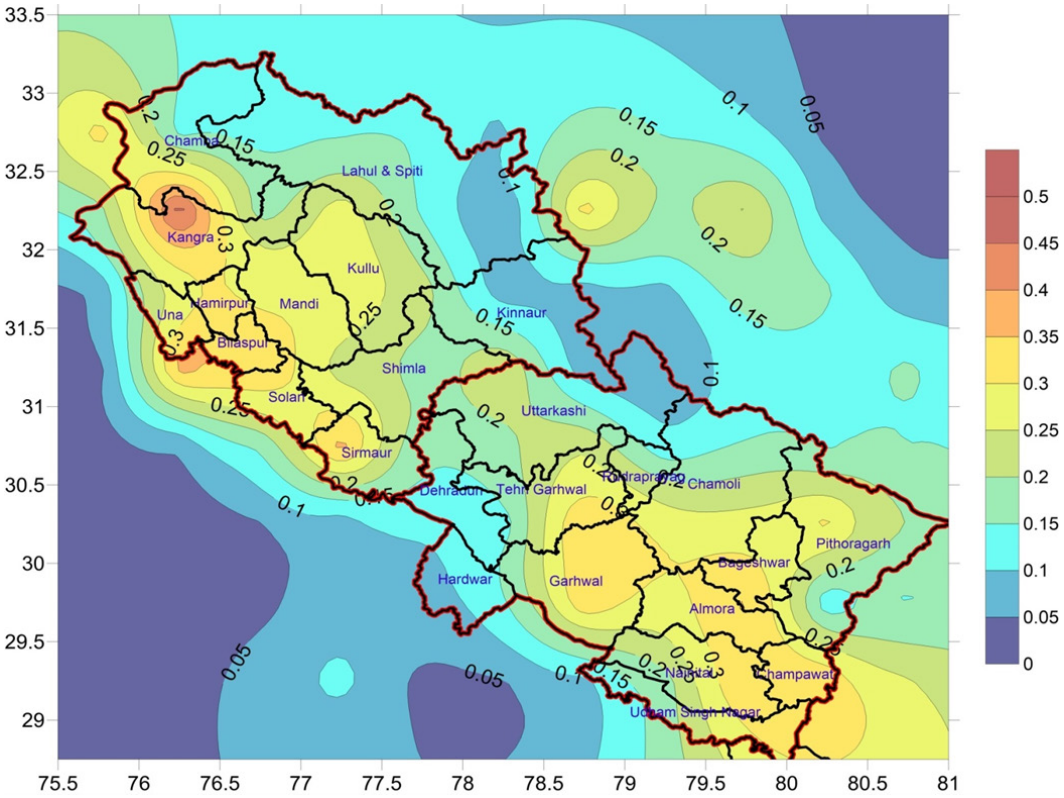

Figure 3. Contour map showing variation of peak horizontal accelerations in the study region

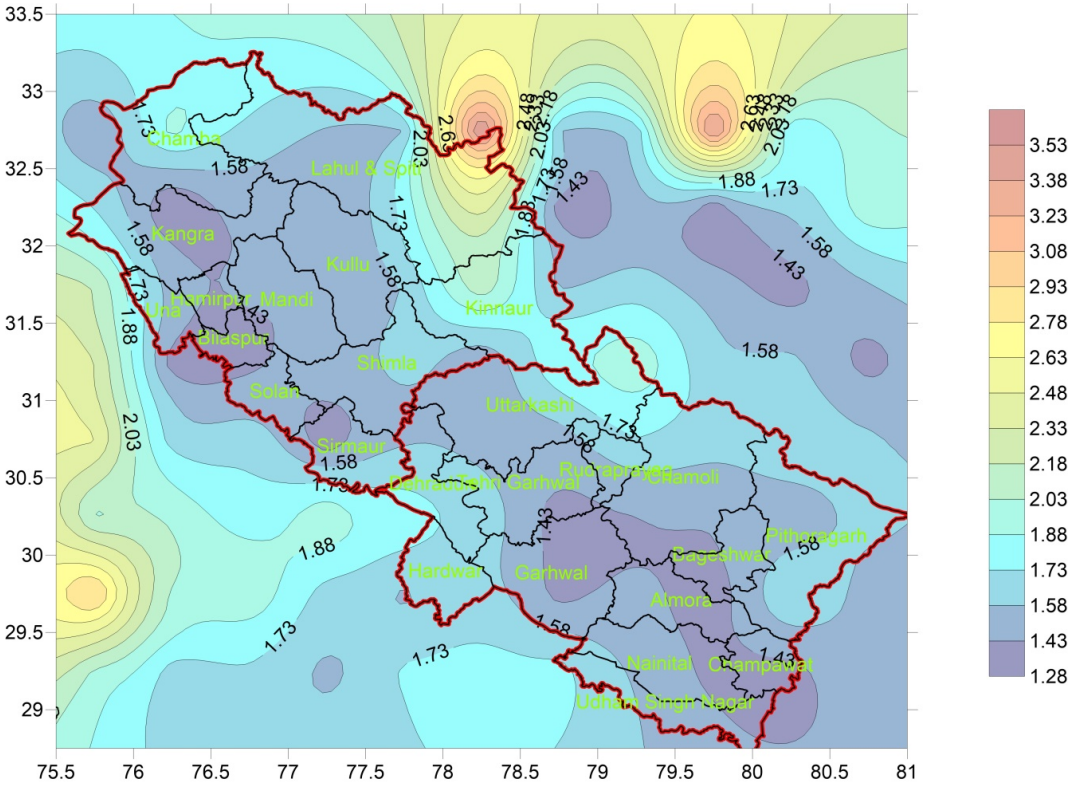

Figure 4. Contour map showing variation of ratio of Horizontal to vertical accelerations in the study region

The contour maps showing the variation of peak horizontal accelerations (a_h) and peak vertical accelerations (a_v) are shown in Figures 2 and 3. The present, study region, Himachal Pradesh (HP), and Uttarakhand, is a northern state in India situated in the western part of the seismically active Himalayan region. This region has experienced several major earthquakes in the past, namely, the Kangra earthquake (Mw 7.8, 1905) with its epicenter in the Kangra region, which resulted in extensive damages to infrastructure and human life. [10] have reported seismic hazard in terms of return periods and probability of earthquake occurrences. Hence, this article presents an estimate estimated of peak horizontal accelerations varying from 0.02g to 0.60g (Figure 1) and peak vertical accelerations vary from 0.01g to 0.47g (Figure 3). The ratios of horizontal to vertical accelerations vary from 3.60 to 1.28 (Figure 4). These estimates would be very helpful for future preparedness planning and even construction practices in the considered area The PGA contour maps prepared for the region show that larger Peak Ground Accelerations are present in the region where there is a higher density of larger faults and vice versa.

[4] Developed a probabilistic seismic hazard map of India and adjoining regions. Eighty six potential seismic source zones were delineated from the earthquake data and major tectonic features, and PGA were computed for 10% exceedence in 50 years in a grid of 0.5° by 0.5°. The values for Himachal Pradesh and Uttarakhand vary from 0.05g to 0.35g. These values are less than those obtained in the present study. The hazard map prepared by [4] is based on large sized source zones and uses different attenuation relationship and thus reflect the broader framework and the values of accelerations may not be representative on local and regional scale as they have not considered the local and regional tectonic features.

ACKNOWLEDGEMENTS

The results presented here is the part of the Master Thesis. Authors are indebted to Department of Earthquake Engineering, IIT Roorkee, Roorkee for providing excellent computational facilities to carry out this research work. Views expressed in this paper are that of authors only, and may not necessarily be of the institute.

REFERENCES

[1] Abrahamson, N.A, Lithehiser, J.J., (1989), "Attenuation of vertical peak acceleration" Bulletin of Seismological Society of America; vol. 79, no.3: 549-567.

[2] Agrawal, P.N., (1991). Engineering Seismology, Oxford & IBH Publishing Co. Pvt. Ltd.

[3] Arya, A.S., (1992). Possible effects of a major earthquake in Kangra region of Himachal Pradesh, Current Science, 62(1-2), 251-256.

[4] Bhatia, S.C., Kumar, M.R. and Gupta, H.K. (1999). A probabilistic seismic hazard map of India and adjoining regions, Annali di Geofisica, 42:1153-1166.

[5] Chandra, U. (1992). Seismotectonics of Himalaya, Current Science, 62 (1–2), 40–71.

[6] Campbell, K. W., (2003). Prediction of strong ground motion using the hybrid empirical method and its use in the development of ground –motion (attenuation) relations in Eastern-North America; Bulletin of Seismological Society of America, 93 (3), 1012-1033.

[7] G S I. (2000), "Seismotectonic Atlas of India and Its Environs". Geological Survey of India, SEISAT 5, 6.

[8] Jain, S. Murthy, C. “Proposed draft provisions and commentary on Indian seismic code IS 1893(Part I)”. IITK-GSDMA-EQ 05- V 4.0.

[9] Kramer, S.L., (1996). Geotechnical earthquake engineering. Prentice Hall international series, Pearson education, Inc, Low price edition, Delhi.

[10] Shubham and D. Shanker (2018). Earthquake Hazard Update in Central Himalaya, Geosciences 8 (1), 1-6.

[11] Valdiya, K.S., (1976). Himalayan transverse faults and folds and their parallelism with subsurface structures of noth Indian Plains; Tectonophysics, 32, 353-386.

[12] Valdiya, K.S. Rana, R.S. and Sharma, P.K., (1992). Active Himalayan Frontal fault, Main Boundary Thrust and Ramgarh Thrust in Southern Kumaun; Jour. Geol. Soc. India, 40, 509-528.

[13] Wells, D.L., and K.J., Coppersmith, (1994). New empirical relationship among magnitude, rupture length, rupture width, rupture area, and surface displacement; Bulletin of Seismological Society of America, 84 (4), 974-1002.